CHAPTER 27

Dimensional Instability Under Irradiation

27. Dimensional Instability under Irradiation

27.1. Introduction

It is a common observation that fuel assemblies and other materials change dimensions during in-reactor service. These dimensional changes consist of permanent plastic deformation suffered by the material when exposed to the reactor environment. The consequences of dimensional instability include the cracking of fuel, pellet-cladding interaction and the failure of rods. Some of these dimensional changes are well known and allowed for in fuel rod design to burnups of 30-40 GWd/ton. However, the operation of fuel to higher burnup and other more severe conditions of operation could again cause dimensional instability to be of concern in light water reactors. In other types of reactors, these dimensional instabilities can be life-limiting. In CANDU reactors, the creep and growth of pressure tubes could cause tube sagging and mandate re-tubing. Void swelling is a serious problem in the stainless steel fuel cladding used in breeder reactors and in the proposed first wall alloys for fusion reactors.

In-reactor dimensional changes can be caused by chemical reactions, such as corrosion and hydriding, or can be caused by irradiation-related processes. Of the changes caused by irradiation, some are caused by irradiation induced phase transformations, (such as amorphization, irradiation-induced precipitation and dissolution of second phases), and which can lead to an observed change in macroscopic dimensions of the material. However, in this chapter we will set aside these dimensional changes caused by changes in chemistry and by phase transformations; we will concentrate only on these changes that are directly related to radiation exposure, occurring in a *single phase material*, that does not suffer macroscopic failure and does not undergo significant changes in chemical composition. However, we need to keep in mind that the actual strains measured in the materials exposed to the reactor environment are a combination of strains caused by all these processes.

The irradiation enhanced or irradiation induced processes that can lead to changes in material dimensions upon reactor exposures are:

- *Irradiation Growth*
- *Void Swelling*
- *Irradiation Creep*

These three processes are caused by different microstructural mechanisms and have different characteristics as illustrated in Figure 27.1. *Irradiation Growth* refers to a change in shape of an unstressed anisotropic material, occurring only under irradiation, and caused by the interaction of point defects with microstructural sinks. *Void Swelling* refers to an isotropic volume increase in an unstressed material caused by the formation of voids inside the material resulting from the agglomeration of point defects and gas atoms. *Irradiation Creep* refers to a slow deformation at constant volume, in a material that is subjected to a stress below the yield stress; the role of irradiation is to accelerate creep mechanisms that occur outside irradiation.

Table 27.1 Characteristics of dimensional changes of metals due to neutron irradiation

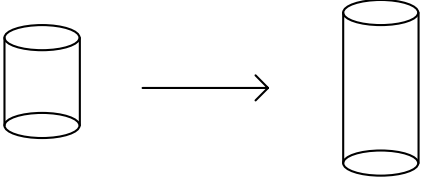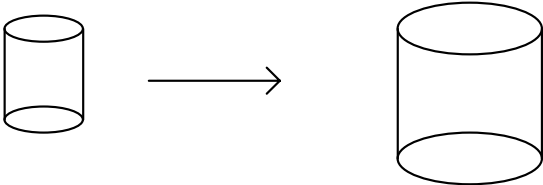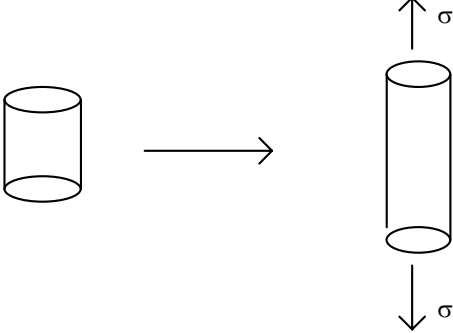| Process	Applied Stress	Crystal structure	Strain	Reversible?	Cause
Growth	None	Anisotropic (hcp, bct, etc)	Anisotropic; constant volume	No	Point defect anisotropic absorption at sinks
Creep	anisotropic	any	Anisotropic as determined by applied stress	No	Stress driven clim and glide of dislocations
Swelling	Any or none	Any; more prevalent in cubic metals, especially fcc	Isotropic volume increase	Yes	Formation of voids from agglomeration of point defects and gas atoms

Irradiation Growth • change in shape • constant density • unstressed	
Irradiation Swelling • increase in volume • decrease in density	
Irradiation Creep • change in shape • constant density • under stress $\sigma < \sigma_y$	

Figure 27.1: **Schematic showing the different types of dimensional instability under irradiation and their characteristics.**

In chapters 9 and 10, we reviewed the process of defect creation, recombination, clustering and absorption at sinks. We have seen that when a material is subjected to the high displacement rates caused by irradiation, the steady state reached by the material (when the defect annihilation rate at sinks equals the production rate) is associated with substantial supersaturations in defect concentrations relative to thermodynamic equililbrium. Given that each atom in the cladding of a nuclear reactor is displaced an average of 10^{-7} dpa.s^{-1} (or about ten times during three reactor years), large defect fluxes to sinks result, such that even minute imbalances in the rates of interstitial and vacancy annihilation at different sinks will cause a net flow of one or the other defect into the sinks. This can lead to internal redistribution of atoms, leading to enhanced deformation and dimensional instability. In this chapter we show how these processes lead to macroscopic changes in the dimensions of materials and using rate theory to derive simple models that describe these processes.

27.2 Irradiation Growth

The growth of anisotropic materials under irradiation is a process that, although unique to the irradiation environment, can also be observed during thermal cycling of anisotropic materials [1]. As we show in the following sections, irradiation growth requires (i) an irradiation flux, (ii) a crystallographically anisotropic material and (iii) that the crystal anisotropy be macroscopically manifest in the as-fabricated component. Irradiation growth strains can reach hundreds of percent and do not appear to saturate.

Further research indicated that irradiation growth occurs by a preferential interaction of irradiation-induced defects with anisotropic sinks in the material. Therefore one of the preconditions for irradiation growth is that the crystal structure of the material be anisotropic (i.e., not cubic, but hexagonal or lower order). Irradiation growth has been observed in anisotropic materials such as orthorhombic uranium and hexagonal-close packed zirconium (growth also occurs in other hexagonal materials, such as zinc and cadmium metal) but not in cubic materials, such as iron. In reality, two kinds of anisotropies are needed for growth to occur, a *microscopic anisotropy* (relative to the crystal structure) and a *macroscopic anisotropy* or *texture* (relating the orientation of the crystal planes to some macroscopic orientation such as the rolling direction) as can result from processing [see Chapter ##).

Two of the anisotropic materials that undergo irradiation growth and are of interest to the nuclear industry are metallic uranium and zirconium alloys. These are reviewed in the following sections.

Irradiation Growth in Metallic Uranium

In the early days of development of nuclear power, metallic uranium was considered as a candidate for nuclear fuel [see papers in the International Conference on Peaceful Uses of Nuclear Energy, Geneva, 1955]. Metallic uranium has several advantages compared to the now standard uranium dioxide, most notably its high fissile atom density, and its high thermal conductivity, which allows operation at a lower fuel centerline temperature. However, early experiments with irradiation of metallic uranium fuel showed that the material underwent a pronounced change of shape under neutron irradiation, growing in particular macroscopic directions and shrinking in others, at nearly constant volume. Since the strains thus obtained could be substantial (on the order of several hundred percent), this was a serious problem, which contributed to the abandonment of metallic uranium as a candidate fuel for power reactors (as mentioned in chapter **, another factor that led to the abandonment of metallic uranium as a candidate fuel was the potential for exothermic chemical reaction between uranium and coolant water and which was one of the contributing factors in the Windscale accident).

Figure 27.2 shows a sample of single crystal metallic uranium before and after neutron irradiation (0.1% burnup). The sample length has increased considerably in the axial direction, (parallel to the [010] direction in the orthorhombic crystal) and its circular

cross section has become elliptical, with the short axis of the ellipsis being the direction parallel to [100] direction in the crystal. Thus the crystal grows in the 010 direction, shrinks in the 100 direction, and remains constant in the 001 direction. At first glance the change observed is very puzzling, as there is no stress applied on the solid, and yet a considerable macroscopic deformation is achieved.
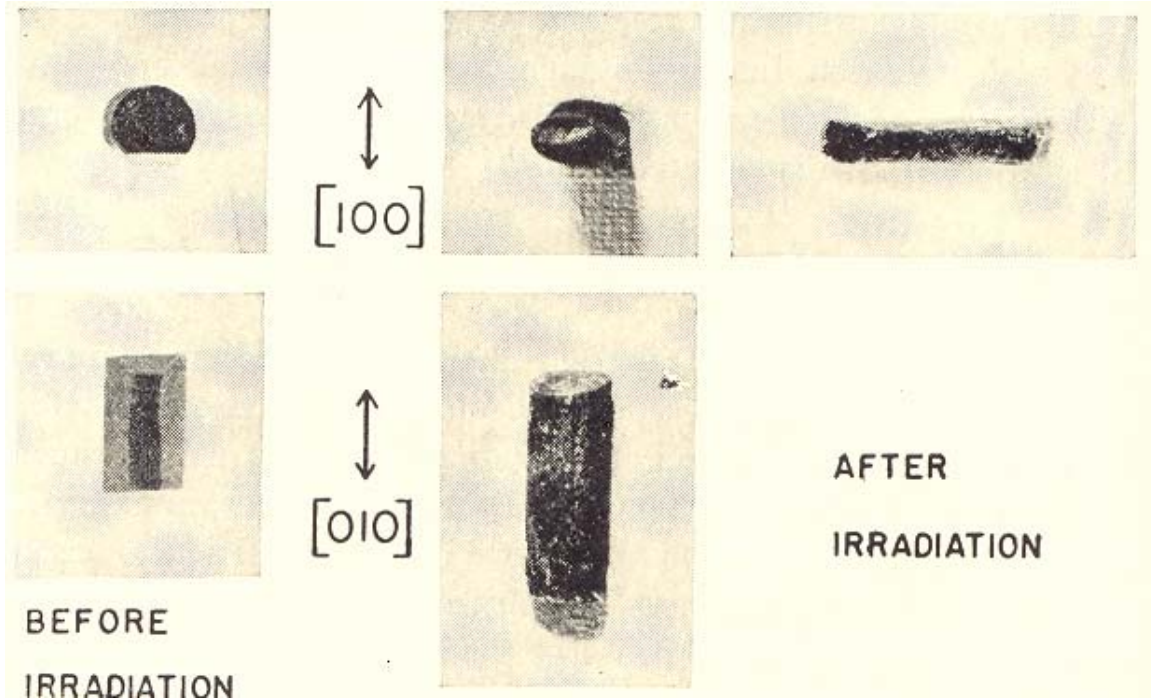
Fig. 27.2 Cylindrical single crystal of alpha-uranium before and after irradiation in a reactor (0.1% atom burnup) [from reference [2], as reported in [1]]

Irradiation growth was initially measured empirically by the growth coefficient g, defined by the formula:

$$\ell_{010}(\beta) = \ell^o_{010} \exp(g\beta)$$
$$\ell_{100}(\beta) = \ell^o_{100} \exp(-g\beta)$$

where β is the burnup

$$g = \frac{1}{\beta}\ln\left(\frac{\ell}{\ell^o}\right) \cong \frac{1}{\beta}\frac{\Delta\ell}{\ell^o}, \text{when } \Delta\ell = \ell^o - \ell \text{ is small} \tag{27.1}$$

Because there is no change in volume during irradiation growth,

$$\varepsilon_{100} + \varepsilon_{010} + \varepsilon_{001} = 0; \qquad \varepsilon_{100} = -\varepsilon_{010} \tag{27.2}$$

Buckley proposed a qualitative model for irradiation growth in uranium [3, 4], based on the preferential condensation of displacement cascades in particular crystallographic planes, as shown in Figure 27.3. Thus, as a direct result of the displacement cascades, and without any need for further thermal diffusion, the defects separate themselves, with the vacancies condensing on the 100 planes and the interstitials on the 010 planes.

Fig. 27.3: Scheme proposed by Buckley to explain irradiation growth in metallic uranium [3]. The anisotropic collapse of vacancy defect clusters on [110] planes coupled to the formation of interstitial clusters on [010] planes, occurring within the displacement cascade leads to a macroscopic strain.

One of the curious factors observed in the growth of uranium is that the growth coefficient actually increases with decreasing temperature, as shown in figure 27.4. This means that the growth is effected by a mechanism that does not depend on the thermal migration of point defects to sinks. Although Buckley's model does not explicitly rationalize the temperature dependence of the growth coefficient, one can imagine that the athermal process described above and present at very low temperature, starts to compete with thermal rearrangements at higher temperatures thus slowing the growth rate. As we will see below, this is not necessarily the case for Zr alloys.
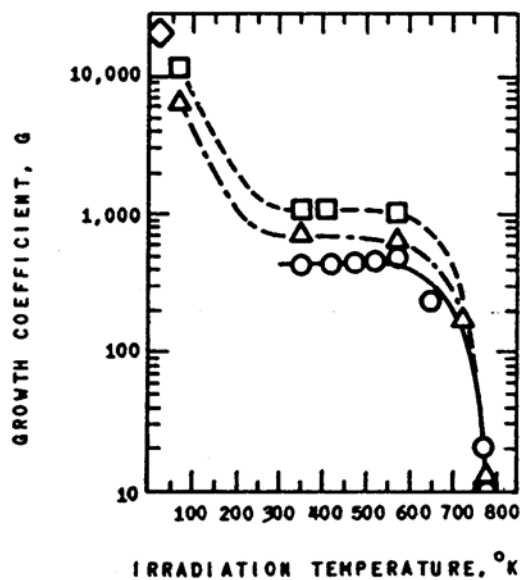
Fig. 27.4: The growth coefficient of uranium metal as defined in equation 27.1 [4].

Of greater interest to the nuclear industry is the irradiation growth of Zr alloys, which we review in the next section. We also use this material to introduce a quantitative model that illustrated the general principles governing irradiation growth.

Irradiation Growth in Zirconium alloys.

Figure 27.4a shows the irradiation growth exhibited by Zr-5% and 7% Pu alloys, when irradiated at 500 C to atom burnups from 0.8 to 1.8% [5]. The plutonium was inserted to create a high displacement rate, and to give a high total dose to the material. The length change is remarkable (the strain is on the order of 400%, with very small density variation). Although the total displacements in this case are several orders of magnitude higher than fuel cladding should normally be subjected to in-service, this experiment illustrates dramatically the process of irradiation growth.

Figure 27.4a: Appearance of Zr-Pu samples before and after neutron irradiation, showing extensive irradiation growth. (a) Non-irradiated sample, (b) Zr-5%Pu, post-irradiation and (c) Zr-7%Pu, post-irradiation [5].

 For Zr single crystals, irradiation growth consists of an expansion along the <a> or prism directions, with a corresponding contraction along the c-axis, as shown in figure 27.5. As the figure shows, the axes along which expansion occurs during irradiation correspond to the axes of minimum thermal expansion and those along which contraction occurs are the

Fig. 1. Typical preirradiation appearance of Zr-Pu alloy specimens. 2 ×.

Fig. 2. Typical postirradiation appearance of Zr-5 wt % Pu fuel specimens. 2 ×.

Fig. 3. Postirradiation appearance of Zr-7 wt % Pu fuel specimens. 2 ×.

axes of maximum thermal expansion, both for U and Zr.

NEED BETTER COPY OF THE PICTURE

AXIS OF MAXIMUM THERMAL [0001]
EXPANSION AND AXIS OF
CONTRACTION DURING
IRRADIATION.

(10) PLANES.

ORTHORHOMBIC UNIT CELL.

CORRUGATED
(010) PLANE

(1010) PLANE

[010]
AXIS OF MINIMUM THERMAL EXPANSION
AND AXIS OF ELONGATION DURING
IRRADIATION.

[100]
AXIS OF MAXIMUM THERMAL EXPANSION
AND AXIS OF CONTRACTION DURING
IRRADIATION.

[1120]
AXIS OF MINIMUM THERMAL
EXPANSION AND AXIS OF EXPANSION
DURING IRRADIATION IN Zn, Cd, Zr & Tl.

(a)   (b)

Fig. 27.5: The crystallography of growth in hexagonal (zirconium) and orthorhombic (metallic uranium) single crystals, showing the axes along which contraction and expansion occur [3].

As shown in Fig.27.5, in zirconium alloys, ε_{0001} is negative, while $\varepsilon_{10\bar{1}0}$ is positive.

The conservation of volume equation for a Zr single crystal is written:

$$\varepsilon_{0001} + \varepsilon_{10\bar{1}0} + \varepsilon_{01\bar{1}0} = 0 \qquad (27.3)$$

which means that $\varepsilon_{0001} = -2\varepsilon_{10\bar{1}0}$

In polycrystalline materials the material texture is what translates the change of shape in the single crystals into a macroscopic strain. For a polycrystalline sample the growth strain in macroscopic direction x, ε_x is related to the single crystal strain by:

$$\varepsilon_x = \varepsilon_g (1 - 3 F_x)$$

where F_x is the resolved fraction of basal poles aligned with macroscopic direction x and ε_g $(=-\dfrac{\varepsilon_{0001}}{2})$ is the growth strain of the single crystal. F_x is the Kearns texturefactor, defined in Chapter **. Thus, a single crystal with one of the prism poles aligned with x, (F_x=0) would exhibit the growth strain ε_g, and a single crystal aligned with the basal poles in direction x (F_x=1) would show a negative growth strain of -2 ε_g. A randomly oriented polycrystal (F_x=1/3) would show a growth strain of zero. That is, not only is it necessary for the material to be anisotropic in its crystal structure, but such anisotropy must be translated into a texture in order for there to be a non-zero growth strain. As noted in chapter ** the fabrication process of Zr alloy components induces a texture, in which, prism poles are preferentially aligned perpendicular to the axial (longitudinal) direction and basal poles are oriented at 30-40 degrees from the radial (normal) direction.

This means that irradiation growth increases the axial length and reduces the thickness of the cladding tube. These changes can cause failure by bowing in restricted rods.

27.2.3. Model for Irradiation Growth

A Quantitative Treatment of The model in Sect. 27.2.3 of Motta Chapter **(DRO MODIFICATION)**

The growth rate in the <a> directions is proportional to the net fluxes of interstitials and vacancies to the <a>interstitial loops and <a> vacancy loops. Per unit volume of metal, the net rate is:

$$Q_{IL}^{net} = \left(Z_I^{aIL}\rho_{aIL} + Z_I^{aVL}\rho_{AVL}\right)D_I C_I - Z_V\left(\rho_{aIL} + \rho_{aVL}\right)D_V C_V \tag{1}$$

where

aIL = <a> interstitial loops on prism planes
aVL = <a> vacancy loops on prism planes

This equation is similar to your Eq (27.8) except that your version does not have the vacancy fluxes to the prism loops. In addition, the terms in the parentheses are added rather than subtracted, as in your Eq (27.8). Is there any reason for this? I would have thought that addition of an interstitial to an <a> loop promotes growth, whether the loop is of the I or V type. Also, it appears that you have equated Z_I^{aVL} to Z_V

Neglecting <c> loops and all network dislocations, the point defect balances are:

$$\frac{K}{\Omega} = \left[Z_V\left(\rho_{aIL} + \rho_{aVL}\right) + k_{gb}\right]D_V C_V \tag{2}$$

where K is the dpa rate and k_{gb} is the grain-boundary sink strength. *The left hand side of (2) is the same as your G in Eq (27.5).*

$$\frac{K}{\Omega} = \left(Z_I^{aIL}\rho_{aIL} + Z_I^{aVL}\rho_{aVL} + k_{gb}\right)D_I C_I \tag{3}$$

Eliminating $D_V C_V$ and $D_I C_I$ from (1) using (2) and (3) and multiplying by Ω to convert to the <a> growth rate gives:

$$\dot{\varepsilon}_g = K\frac{(Z_I^{aIL} - Z_V)k_{gb}\rho_{aIL} + (Z_I^{aVL} - Z_V)k_{gb}\rho_{aVL}}{\left[Z_I^{aIL}\rho_{aIL} + Z_I^{aVL}\rho_{aVL} + k_{gb}\right]\left[Z_V(\rho_{aIL} + \rho_{aVL}) + k_{gb}\right]} \tag{4}$$

If $Z_I^{aVL} \cong Z_V$ and all bias factors in the denominator are approximated by unity, (4) reduces to:

$$\dot{\varepsilon}_g = K \frac{k_{gb}\rho_{aIL}}{\left[(\rho_{aIL} + \rho_{aVL}) + k_{gb}\right]^2}(Z_I^{aIL} - Z_V) \qquad (5)$$

The components of this "three-factor" formula are:
- the displacement production rate K
- The sink strength balance term
- The loop bias factor difference

The mechanism of irradiation growth in Zr alloys is the partitioning of point defects to different microstructure sinks that align themselves preferentially with particular crystallographic directions. We have shown in Chapter ** that the neutron irradiated microstructure of Zr alloys consists of a mixture of both vacancy and interstitial <a> loops. At steady state, according to equation ***, the overall flux of interstitials and vacancies to sinks, J_I and J_v are equal to each other and to the displacement rate G:

$$J_{Ii} = J_i^{<a>inters.loops} + J_i^{<a>vac.loops} + J_i^{grain\ boundaries} +$$
$$+ J_I^{<c>.loops} + J_I^{<c+a>networkd\ dislocation} + ... = J_v = G \qquad (27.5)$$

The precondition for irradiation growth to occur is for there to be a net flux of one of the defects to an oriented sink. NEED TO EXPLAIN c and c+a loops For example, if interstitials are preferentially absorbed at <a> loops, and they interact more strongly with interstitial loops than vacancy loops, then:

$$J_i^{<a>inters.loops} > J_i^{<a>vac.loops} \qquad 27.6$$

This imbalance in the defect fluxes needs to be compensated at another sink so that steady state condition is satisfied. Thus, if vacancies are produced at the same rate as interstitials then they need to be absorbed preferentially in a neutral (non-oriented) sink, such as grain boundaries. This exactly compensates the imbalance in interstitial absorption at <a> loops so that equation ** is satisfied, i.e.

$$J_v^{grain\ boundaries} - J_I^{grain\ boundaries} = J_I^{<a>int.loops} - J_I^{<a>vac.loops} \qquad (27.7)$$

The growth strain will then be proportional to this imbalance in defect absorption, or

$$\varepsilon_g \propto J_I^{<a>int.loops} - J_I^{<a>vac.loops} = (z_I\rho_{<a>int.loops} - z_v\rho_{<a>vac.loops})D_IC_I \qquad (27.8)$$

If the interstitial and vacancy dislocation loop densities are approximately equal, then the growth strain will be proportional to the difference in dislocation bias factors for interstitials and vacancies (z_I- z_v). In this scenario, the vacancy and interstitial fluxes to the oriented sinks work mostly at odds with each other so that it is the only the *difference*

between the two fluxes to the <a> dislocation loops that causes the observed strain. This model is approximately valid for recrystallized material at low fluences.

In cold-worked material, the growth rates can be much higher. This is shown in Figure 27.6, which plots the growth strain versus temperature for both cold worked and recrystallized material [6].
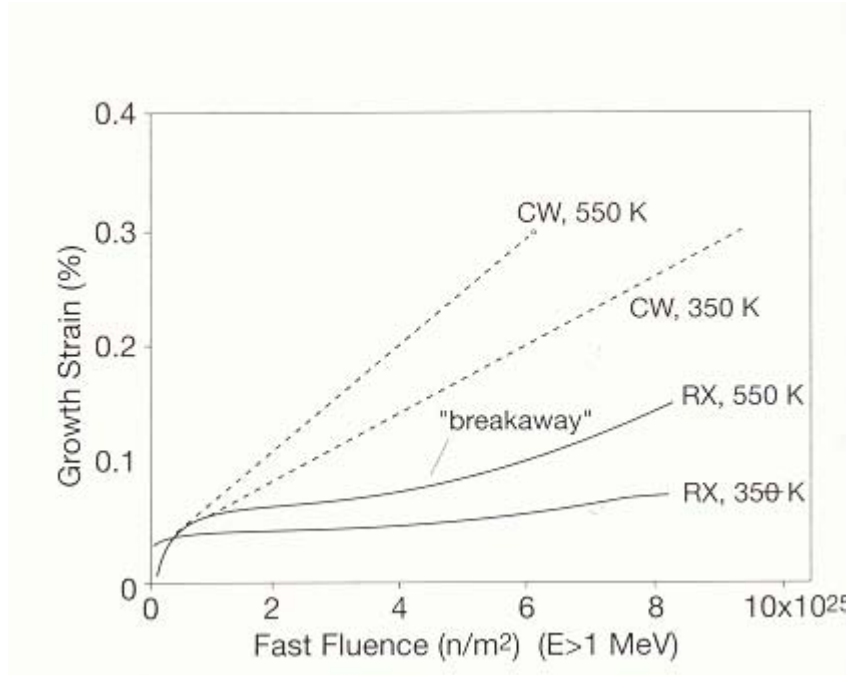

Figure 27.6: Growth strain as a function of neutron fluence for Zircaloy, in the cold-worked and recrystallized states at reactor temperature and room temperature.

This is because cold worked material exhibits a density of $<c+a>$ network dislocations from the start of the irradiation. This means that interstitials are absorbed in $<a>$ loops thus increasing the material dimensions in that direction, while vacancies are absorbed in $<c>$ component loops or network ($<c+a>$) dislocations, which effectively means that both defect fluxes now contribute to the growth strain. i.e.:

$$\varepsilon_g \propto J_i^{<a>\text{int}.loops} + J_v^{<c+a>vac.loops}$$

Because of this the growth strain in cold worked material is normally higher than that in recrystallized material at the start of irradiation. However, at higher fluences (around 3-4 x 10^{25} n.m^{-2}) other types of loops showing a component in the $<c>$ direction start to appear, and the material starts to behave like cold worked material. This is what is termed accelerated or breakaway growth [6] [7].

According to Woo [8], the reason for the partitioning of the different defects to different sinks is the migration anisotropy of these defects in the zirconium crystal structure. They have proposed a model that states that since there is a diffusion anisotropy difference

(DAD), the vacancies tend to migrate in the 0001 direction, while interstitials migrate in the perpendicular direction. Because of this, vacancies have a greater probability of interacting with dislocations whose habit planes are in the basal plane than in prism planes, causing the observed bias. <mark>MORE DETAILED EXPLANATION/DIAGRAM for DAD</mark>

27.3 Void Swelling

The phenomenon of void swelling was discovered by Cawthorne and Fulton [9], who attributed it to the formation of cavities in solids during irradiation. The phenomenon can be observed with the naked eye in Figure 27.7a, which depicts the change in dimensions undergone by stainless steel after a high fluence irradiation.

(a)   (b)
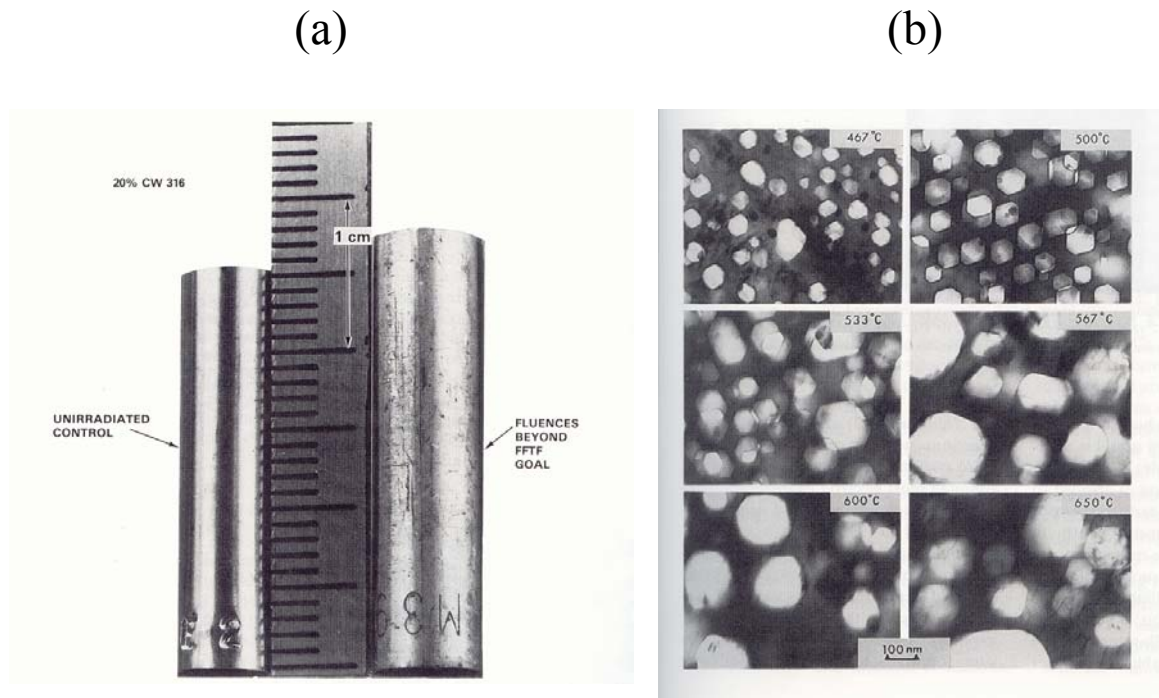
Figure 27.7 (a): Swelling observed after irradiation to 1.5 x 1023 n.cm-2 (E >0.1 MeV) at 510 C in EBR-II (or equivalent to about 75 dpa) [10];. (b) TEM micrographs of voids formed in 316 stainless steel, during irradiation at various temperatures in FFTF (Fast Flux Test Facility) to a fluence of 1.4 x 10^{23} n.cm^{-2} (W.J.S. Yang picture, from reference [11]).

Since the number of transmutation He atoms formed during irradiation is considerably less than necessary to explain the observed strain, these cavities had to be mostly constituted of vacancies, and hence the name void swelling. Figure 27.7b shows transmission electron micrographs depicting the evolution of voids formed during neutron irradiation of stainless steel. It is clear from the pictures that voids increase with irradiation and the void growth does not saturate.

Because void swelling was observed in stainless steel, which was to be used for fuel cladding in fast breeder reactors, there was considerable impetus, especially in the 1970s to perform research in this area. Also the swelling of uranium dioxide during reactor exposure, is of great technological interest, since it affects fission gas release (see chapter **) and can cause pellet-cladding interaction. Such research has uncovered many of the basic mechanisms of void swelling. We review some of these in the following section.

Mechanism of void swelling

The microscopic mechanism of void swelling is the formation of small cavities in the solid, perhaps with a little gas in them, which helps stabilize the void embryos. Most metals undergo void swelling under neutron irradiation, in the range of 0.3 to 0.55 of the melting temperature. One of the pre-conditions of swelling is the existence of some gas in the material.

Voids form by the condensation of vacancies into clusters, which can then grow by net vacancy absorption or by coalescence with other voids. We can divide this process into one of void nucleation and void growth.

Void Nucleation

In chapter ** we described the nucleation of a second phase from a solid solution. We showed that nucleation of a second phase occurs when a nucleus of a critical size is formed above which it is more probable for the nucleus to grow than to shrink, and thus a stable nucleus is formed. In the case of neutron irradiation the nucleation of voids can occur *homogeneously* (i.e. two vacancies coalesce and form a divacancy which grows by one vacancy at a time by the slow accretion of vacancies and gas atoms) or *heterogeneously* (e.g., a displacement cascade directly creates multi-vacancy clusters which may even be beyond the critical radius, or vacancies and gas atoms agglomerate at grain boundaries or precipitate interfaces such that the surface energy is reduced and nucleation is facilitated). In the case of uranium dioxide such gas is present in the form of fission gas. In the case of iron based alloys the transmutation reaction $Fe(n,\alpha)$ causes the formation of helium gas which can help stabilize the voids. By contrast in Zr alloys, in the absence of sources of transmutation gas, no void swelling is observed. If however, Zr is pre-injected with gas, then cavities do form [12].

The presence of insoluble gas atoms in the void helps stabilize the voids against dissolution, because once the void is dissolved, the gas atoms have to return to solution, which is energetically unfavorable.

NEED A nucleation reference
[Formulation of nucleation problem; Don, here we have to decide what to use; your derivation in pages 106-110 of the 220 notes is interesting, but I am not sure if it illustrates physically what happens in the solid; from what I understand it takes a group of clusters through the critical radius, taking into account emission and absorption of the

Void Growth

The vacancy clusters resulting from the nucleation process will grow at rates that depend on the relative rates of the following processes:

i. cluster growth by vacancy absorption
ii. cluster shrinkage by vacancy emission
iii. cluster shrinkage by interstitial absorption.

After the nucleation process is finished, then void growth predominates, with the total density of voids *N* remaining approximately constant. If we approximate the void distribution to the total density of voids at the average size *R,* we obtain:

$$\frac{\Delta V}{V} \approx \frac{4}{3}\pi R^3 N \qquad\qquad 27.12$$

Thus once we have solved the nucleation problem to find the total number of voids *N* we need to calculate $\overline{R}$ as a function of fluence to obtain the void swelling strain *ΔV/V*. Since at steady state the rate of vacancy and interstitial elimination at sinks needs to be the same, and voids are *neutral* sinks, in order for there to be void growth (net flow of vacancies to voids) there needs to be a corresponding net flow of interstitials to another sink, e.g., dislocations. This is why void swelling and irradiation creep can be coupled phenomena. Figure 27.9 shows the partition of defects into different sinks that is necessary to obtain measurable strain.
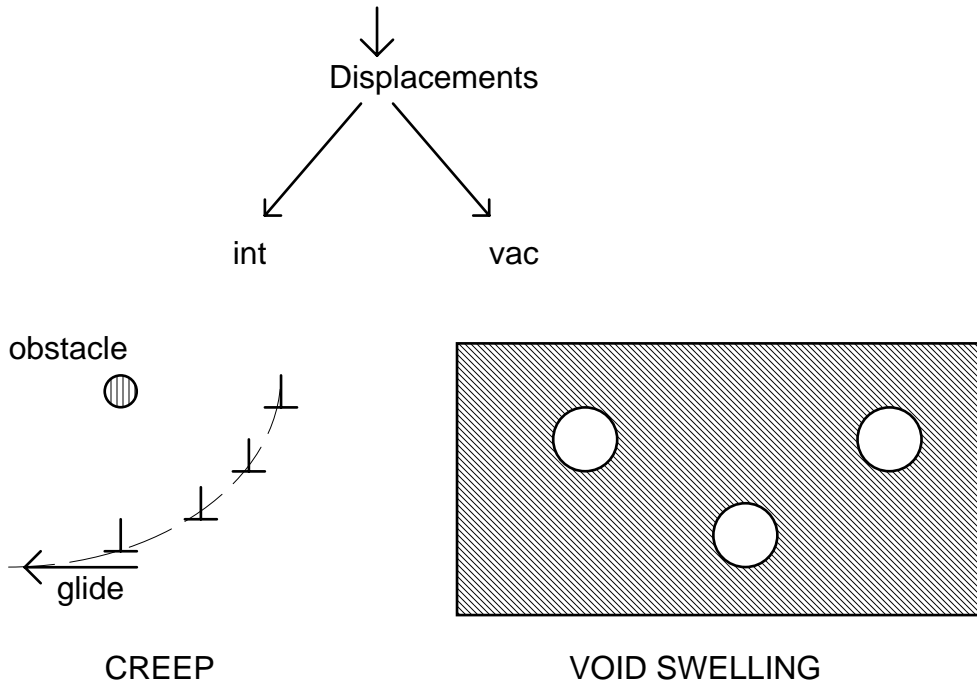
Figure 27.9: The coupling of irradiation creep and void swelling. As displacements are produced the interstitials are preferentially absorbed at dislocations and as a result a net flow of vacancies arrives at the voids, causing them to grow.

With the simplification shown in equation 27.12 we have to solve only the growth law for a single void. The fractional variation in void volume is given by:

$$\frac{d}{dt}\left(\frac{4}{3}\pi R^3\right) = \left(J_v^{void} - J_I^{void}\right)$$

27.13

If C_v^{eq} is small compared to C_v, then we can write:

$$4\pi R^2 \dot{R} = \left(4\pi R D_v C_v - 4\pi R D_I C_I\right)$$

27.14

$$\dot{R} = \frac{\left(D_v C_v - D_I C_I\right)}{R},$$

27.15

If we insert the general solution of the steady-state rate equations, given in equation 13.xx. into 27.14, we obtain:

$$D_I C_I = \frac{D_I D_v}{2K_{Iv}} \sum_j S_{jv}\left[-1 + \left(1 + \eta\right)^{1/2}\right]$$

27.16

10/5/2006   1

$$D_v C_v = \frac{D_I D_v}{2K_{Iv}} \sum_j S_{jI} \left[-1 + (1+\eta)^{1/2} \right] \qquad 27.17$$

$$\text{where} \quad \eta = \frac{4GK_{Iv}}{D_v D_I \sum_j S_{jv} \sum_j S_{jI}} \qquad 27.18$$

and where the $\sum_j S_{jk}$ are the sum of all sink strengths present in the material for defect k.

If only voids and dislocations are present, then:

$$\sum_j S_{jv} = z_v \rho_d + 4\pi RN$$

$$\sum_j S_{jI} = z_I \rho_d + 4\pi RN \qquad 27.19$$

and substituting 27.19 into 27.16, 27.17 we obtain

$$D_v C_v - D_I C_I = \frac{(z_I - z_v)\rho_d D_I D_v}{2K_{Iv}} \left[-1 + (1+\eta)^{1/2} \right] \qquad 27.20$$

Substituting equation 27.20 into 27.15, we obtain $\dot{R}$:

$$\dot{R} = \frac{1}{R} \frac{(z_I - z_v)\rho_d G}{(z_I \rho_d + 4\pi RN)(z_v \rho_d + 4\pi RN)} \frac{2}{\eta} \left[-1 + (1+\eta)^{1/2} \right] \qquad 27.21$$

which can also be written:

$$\dot{R} = \dot{R}_o F(\eta) \qquad 27.22$$

$$\dot{R}_o = \frac{1}{R} \frac{(z_I - z_v)\rho_d G}{(z_I \rho_d + 4\pi RN)(z_v \rho_d + 4\pi RN)}, \qquad 27.23$$

$$F(\eta) = \frac{2}{\eta} \left[-1 + (1+\eta)^{1/2} \right] \qquad 27.24$$

Here $\dot{R}_o$ is the void growth rate without recombination.

$$\eta = \frac{4K_{Iv}G}{D_I D_v (z_I \rho_d + 4\pi RN)(z_v \rho_d + 4\pi RN)} \qquad 27.25$$

If $z_I \cong z_v$ (for the purposes of writing η)

$$\eta = \frac{4K_{Iv}G}{D_{Ii}D_v\left(z_v\rho_d + 4\pi RN\right)^2} = \frac{4K_{Iv}G}{D_I D_v\left(1 + \dfrac{4\pi RN}{z_v\rho_d}\right)^2 z_v^{\,2}\rho_d^{\,2}} \qquad \text{27.26}$$

If we define $x = \dfrac{4\pi RN}{z_v\rho_d}$, then equation 27.23 can be written:

$$\dot{R}_o = \frac{G}{4\pi R^2 N}\left(\frac{z_I - z_v}{z_v}\right)\frac{x}{\left(1 + x\right)^2} \qquad \text{27.27}$$

Equation 27.27 represents the growth rate of a void in the absence of recombination. It is instructive to study how this equation behaves. Notice for example that two conditions need to be satisfied for $\dot{R}_o$ to be different than zero:

(a) There has to be a net bias of interstitials for dislocations (i.e., z_i needs to be different from z_v). This is because there needs to be a driving force for the partitioning of defects, i.e. if both defects arrive at the same rate at a given sink, there is no net flux and no effect.

(b) The sink strengths of dislocations and voids need to be approximately balanced, i.e., x needs to be ≈ 1, otherwise $\dot{R}_o \rightarrow 0$. The reason for that is that if either sink becomes much more numerous than the other, then they dominate defect absorption and thus defect partitioning effectively ceases.

Recombination decreases the overall number of defects available to be absorbed at sinks and therefore decreases the swelling rate. We can evaluate the effect of recombination by examining the function $F(\eta)$:

$$\eta = \frac{4K_{Iv}G}{D_i D_v\left(z_v\rho_d + 4\pi RN\right)^2} \qquad \text{27.28}$$

but from chapter ** $K_{Iv} = K_{Ivo}(D_I + D_v)$. If $D_I \gg D_v$, then

$$\eta \approx \frac{4K_{Ivo}G}{D_v\left(z_v\rho_d + 4\pi RN\right)} = \frac{BG}{D_v}. \qquad \text{27.29}$$

where B is a constant. This means that η decreases with temperature. Recombination tends to be highest when G is high and the temperature is low. Effectively, we can see that this holds: when the temperature is high, η is small and $F(\eta)$ goes to one. When the temperature is low, η is large and therefore $F(\eta)$ is smaller than 1. Thus for those conditions, recombination offsets void swelling.

$$F(\eta) = \frac{2}{\eta}\left[-1 + \left(1 + \eta\right)^{1/2}\right] \qquad \text{27.30}$$

Figure 27.10 shows the value of $F(\eta)$ calculated for various values of η. A few things can be remarked from the graph. When $F(\eta)$ approaches 1, recombination is negligible, and $\dot{R} \approx \dot{R}_o$; when $F(\eta)$ approaches infinity, recombination becomes increasingly important and swelling does not occur.
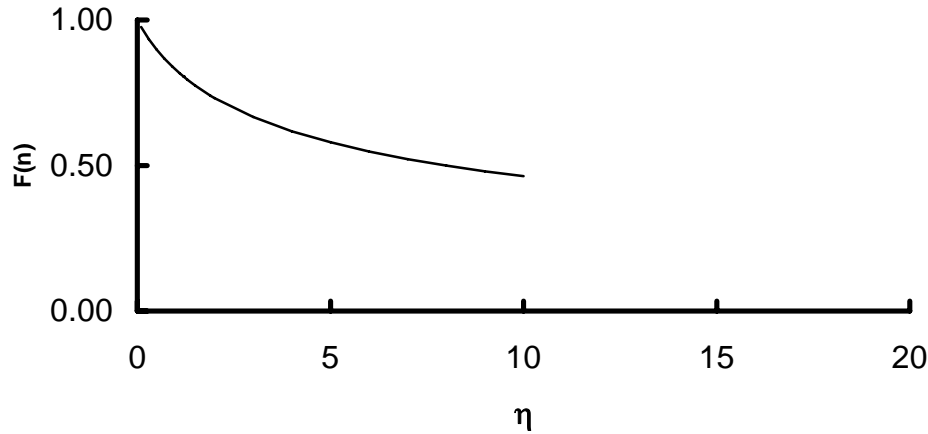

Figure 27.10: The factor $F(\eta)$, as defined in equation 27.30, and calculated for various values of η. As η increases the importance of recombination increases relative to the annihilation of defects at sinks.

At high temperature swelling decreases. This is because thermally activated vacancy emission from voids becomes increasingly important at high irradiation temperatures, and thus limits void growth. We can write this more complete formulation as:

$$\dot{R} = \dot{R}_o F(\eta) + \dot{R}_e \qquad\qquad 27.31$$

where
$\dot{R}_e$ = decrease in void radius resulting from thermal emission of vacancies from voids. This is a thermally activated process which depends on the formation energy of the vacancies and on the cluster binding energy (see chapter **). The point is that there is an *optimal* temperature range for swelling, where there is a balance between void stability from thermal emission and recombination. This is illustrated in the experimental results shown in Figure 27.11. For this particular steel, the swelling strain goes through a maximum at approximately 500 C.

As shown by the equations 27.28 and 27.29, the lower limit of this optimal temperature range for void swelling is partly determined by the damage rate G. In general the higher the damage rate G, the higher the lower temperature limit of void swelling. It has been observed experimentally that in general the void swelling temperature range for ion

irradiation (high dose rate) is higher than for neutron irradiation, qualitatively confirming the observations above.
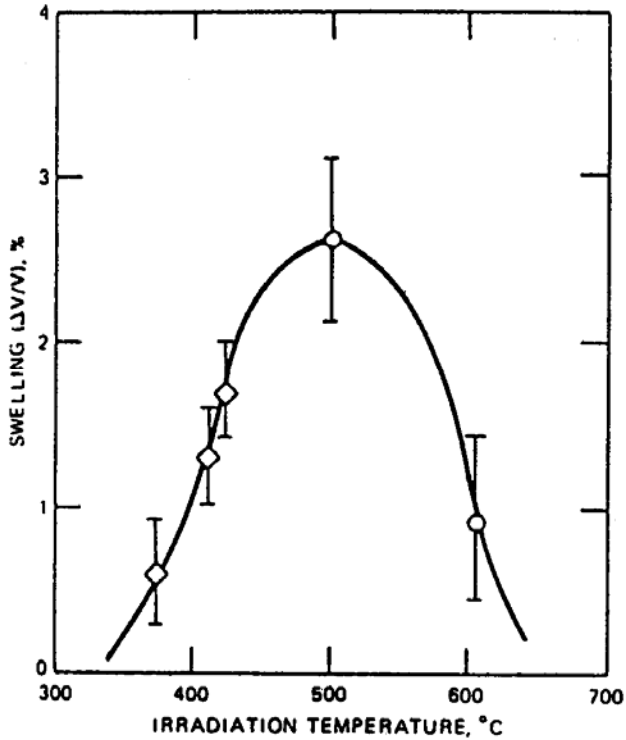

Figure 27.11: Void swelling strain versus temperature for the 304 stainless steel after a neutron exposure of 5 x 10^{22} n.cm^{-2} (E>1 MeV).

27.4 Irradiation Creep

As mentioned in chapter **, the material behavior in a uniaxial tensile test is determined by its stress-strain curve. At stresses below the yield stress the material undergoes only elastic deformation and only above σ_Y does permanent (or plastic) deformation occur. Strictly speaking, this is only true for tests in which the holding time at stress is short. When the material is held at stresses below σ_Y for very long periods of time (weeks, months) plastic deformation can occur by *creep.* Thus, creep is defined as slow plastic deformation, under a stress smaller than σ_Y. Irradiation creep can also have similar consequences as the other deformation mechanisms discussed in this chapter, i.e., failure or bowing due to excessive deformation, but it can also have a beneficial effect in relaxing stresses applied to the solid.

27.4.1.Thermal Creep Mechanisms

Different creep regimes occur in various materials and several thermal creep mechanisms exist such as climb and glide, Coble creep, Nabarro-Herring creep, grain boundary sliding, etc. [13]. Deformation mechanism maps such as shown in figure 27.11a, are a good way of describing the temperature ranges and stresses at which we would expect to see different mechanisms active [14, 15].
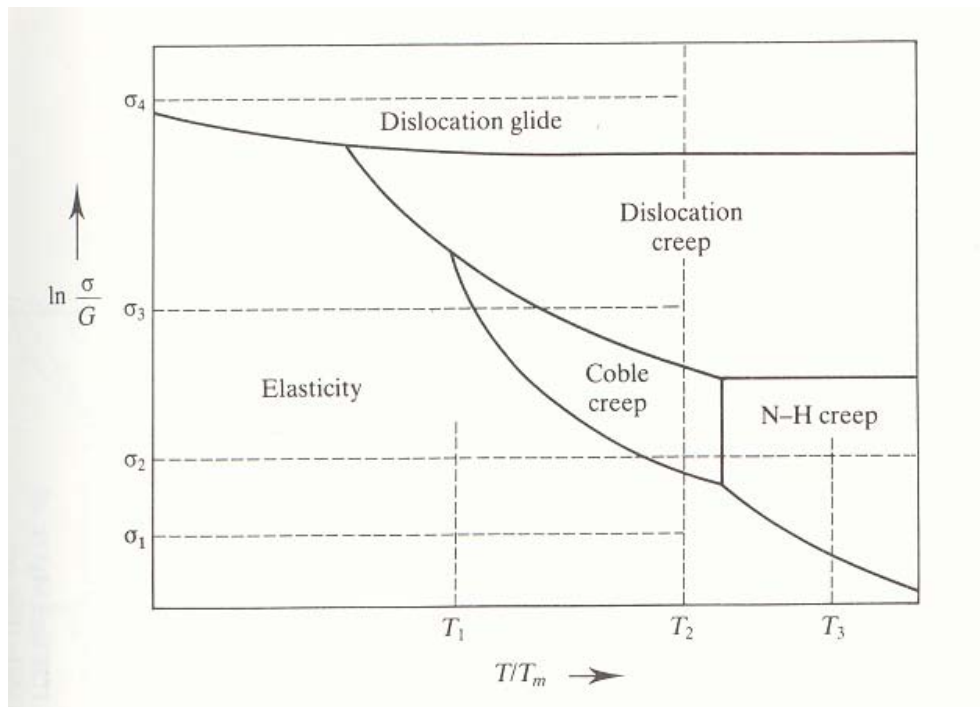

Figure 27.11a: Schematic deformation mechanism map under thermal conditions. The combination of homologous temperature and stress determines the dominant deformation mode; from [13]. GET BETTER EXAMPLE WITH NUMERICAL VALUES

In general, the climb-and-glide mechanism are restricted to high temperature ($T/T_m >$??), where the intrinsic thermal defect concentration is high. Such conditions are mimicked at lower temperatures by the irradiation field. In general, the presence of irradiation enhances the rates of the thermal creep processes, for example by an enhanced diffusion coefficient present under irradiation. Irradiation also enables other mechanisms that can cause or enhance creep.

Irradiation Creep Mechanisms

As mentioned in the previous sections, for all the irradiation processes in the sink dominated regime at steady state, in order to have a measurable strain it is necessary to have a partition of defects to sinks, otherwise the defect fluxes cancel. It is only necessary for *one* of the defects to have a preferential interaction with one of the sinks , as the annihilation of the opposite defect in the neutral sinks automatically increases to match the flux of defects to the preferential sinks. This partition can occur by several mechanisms. The principal class of mechanisms at the root of irradiation creep are the so-called climb-and-glide mechanisms. These mechanisms involve the preferential absorption of interstitials at dislocations, which causes the dislocations to *climb* and enables their *glide*, which causes the creep strain (see chapter ** for thermal mechanisms).

The preferential absorption of interstitials at dislocations can be caused by a variety of reasons. In the stress induced preferential absorption mechanism (SIPA), INSERT SIPA mechanism from NE220 notes [16] an applied stress applied to a solid with randomly oriented dislocations, causes preferential absorption of interstitials in those dislocations that are aligned with the applied stress, thus causing creep in that direction.
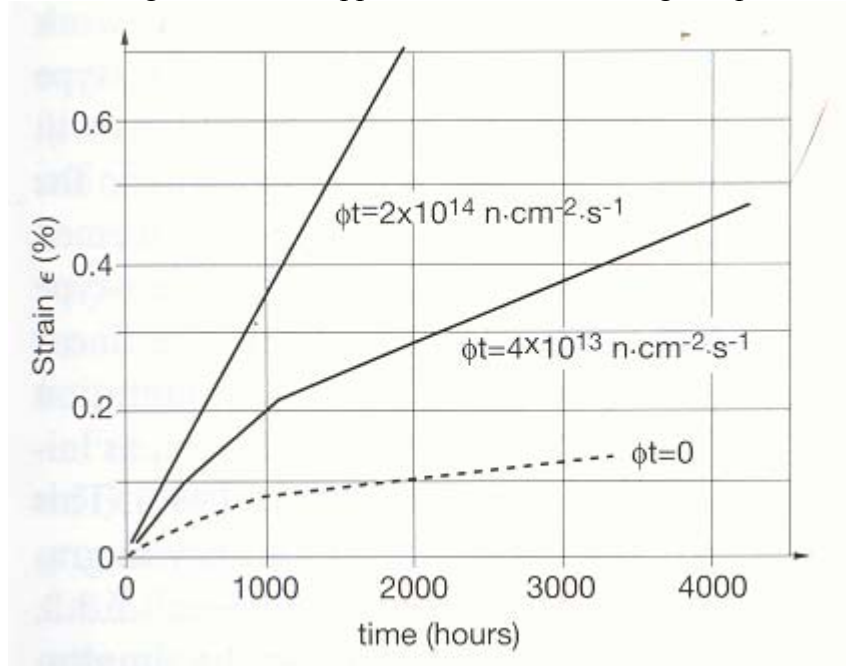
Figure 27.11b: Diametral creep strain for recrystallized Zircaloy (under internal pressure, kept at 330 C), outside irradiation and under irradiation for two values of the neutron flux.

Vacancies in these models can be absorbed by several different sinks, including voids, grain boundaries, and dislocations. This explains why materials that do not undergo void swelling can still undergo creep: vacancies can go to sinks other than voids in these materials. Figure 27.11b shows the creep deformation of Zircaloy outside of irradiation and under irradiation. It is clear that increasing values of the displacement rate G cause ever-increasing creep strains.

In the case of Zircaloy creep, anisotropies in the point defect migration or in defect absorption by different types of dislocations such as the diffusion anisotropy difference (DAD) or stress induced preferential absorption (SIPA) mechanisms mentioned above, have to be invoked to rationalize the creep strain. Also, in anisotropic materials, creep always has to be separated from growth in experimental situations. A convenient way to do this is to assume

$$\dot{\varepsilon}_{total} = \dot{\varepsilon}_{growth} + \dot{\varepsilon}_{creep} \tag{27.32}$$

and define $\dot{\varepsilon}_{creep}$ as the additional deformation that takes place when the external stress is different than zero.

27.4.3 Swelling-Driven Irradiation Creep Model

As illustrated in Figure 27.9, irradiation creep and void swelling can be coupled phenomena. In that case, we have *swelling-driven irradiation creep*. The model presented here for this type of mechanism is valid for steels, where void swelling occurs, but not for Zircaloy. In the case of steels, the creep rate originates in the excess flux of interstitials to dislocations.

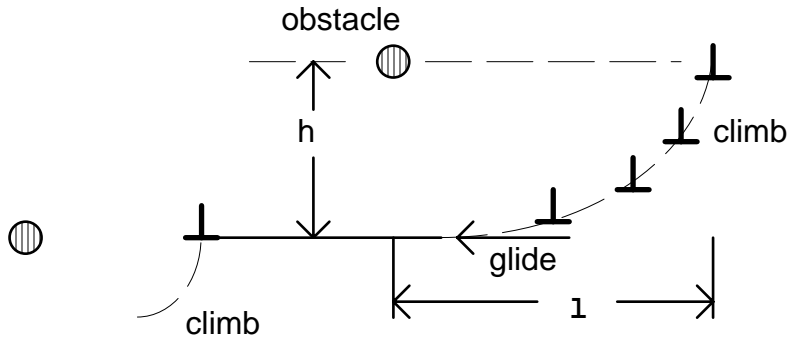The creep strain can be written
$$\dot{\varepsilon} = \rho_d^m b \, \mathrm{v}_d \qquad\qquad 27.33$$

where
$\rho_d^m = \text{density of mobile dislocations (cm/cm}^3)$
$b = \text{Burgers Vector}$
$\mathrm{v}_d = \text{dislocation velocity}$

CREEP

Figure 27.12: The climb and glide mechanism of irradiation creep. A dislocation that is stopped at an obstacle absorbs point defects that allow it to change its plane and thus avoid the obstacle. When enough climb has occurred, glide occurs very quickly.

Dislocation climb is a process that is controlled by defect absorption on dislocations and is therefore limited by the migration rates of defects in the solid. Once the dislocations have climbed enough that they clear the obstacles, glide occurs relatively fast. Because of this we can write that the dislocation velocity is approximately equal to the climb velocity:

$$v_d = \frac{l}{t_c}$$
<div align="right">27.34</div>

$$t_c = (\text{time to climb barrier h}) = h/v_c$$
<div align="right">27.35</div>

where h is the barrier height, determined by the interaction of dislocation with the obstacle, as shown in Chapter **. For example if the obstacle is an immobile dislocation then:

$$h = \frac{\mathbf{G}b}{8\pi(1-\upsilon)\sigma_{xy}}$$
<div align="right">27.36</div>

The climb velocity v_c is calculated by computing the imbalance between the vacancy and interstitial defect fluxes to dislocations.
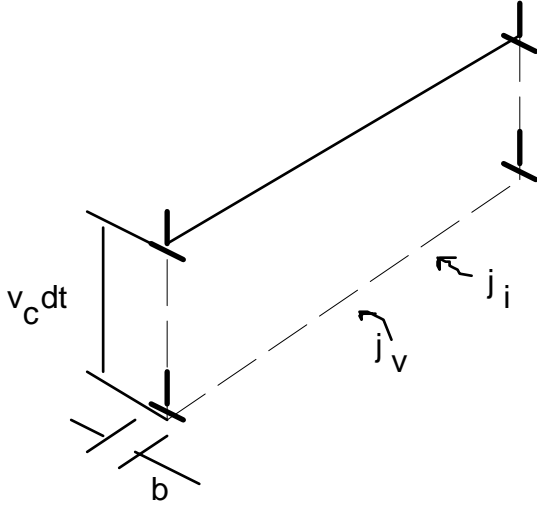
Figure 27.13: The absorption of defects at dislocation causing dislocation climb.

From conservation of mass, in time dt the defect fluxes and the dislocation climb are related by:

$$(j_i - j_v)\,\Omega\, dt = v_c\, b\, dt \qquad\qquad 27.37$$

where Ω is the atomic volume and j_i, j_v=defect fluxes per unit length of dislocation line [defect.s^{-1}.cm^{-1}]

$$v_c = \frac{(j_i - j_v)\cdot\Omega}{b} = \frac{(z_i D_i C_i - z_v D_v C_v)\,\Omega}{b} \qquad\qquad 27.38$$

The total fluxes are related to the flux per unit length by the equation

$$j_i - j_v = \frac{J_i^{dis} - J_v^{dis}}{\rho_d} = z_i D_i C_i - z_v D_v C_v$$

A relationship can be found between void swelling and irradiation creep by imposing the condition

$$J_i^{dis} - J_v^{dis} = J_v^{void} - J_i^{void} \qquad\qquad 27.39$$

But

$$\frac{d}{dt}\left(\frac{\Delta V}{V}\right) = \left(\frac{\Delta\dot V}{V}\right) = \Omega\rho_d(z_i D_i C_i - z_v D_v C_v) = \Omega 4\pi RN(D_i C_i - D_v C_v) \quad 27.40$$

So the climb velocity can be written in terms of the void swelling strain rate

$$v_c = \frac{1}{\Omega\rho_d}\left(\frac{\Delta\dot V}{V}\right)\frac{\Omega}{b} \qquad\qquad 27.41$$

This can now be substituted in the equation 27.33 for the creep strain, remembering that

$$v_d \cong \frac{l}{h} v_c \qquad\qquad 27.42$$

And thus finally

$$\dot{\varepsilon}_{irr} = \rho_d^m b \frac{l}{h} v_c = \rho_d^m l \left(\frac{\Delta \dot{V}}{V} \right) \frac{1}{\rho_d} \frac{8\pi(1-v)\sigma_{xy}}{G_b} \qquad\qquad 27.43$$

$$\dot{\varepsilon}_{irr} = \frac{\rho_d^m}{\rho_d} \frac{8\pi(1-v)l}{G_b} \left(\frac{\Delta \dot{V}}{V} \right) \sigma_{xy} \qquad\qquad 27.44$$

Thus, the in swelling-driven creep by a climb and glide mechanism, the creep rate is directly proportional to the swelling rate, as well as to the applied stress and the fraction of mobile dislocations.

Problems for Chapter 27

27.1. A reactor component is made of steel and it is undergoing irradiation. It is found during post irradiation examination that the material has undergone void swelling, and irradiation creep by a climb and glide mechanism. It is known that the interstitial diffusion coefficient is 10^{-6} cm^2/s and the vacancy diffusion coefficient is 10^{-11} cm^2/s. The material reaches steady state quickly after the start of irradiation. The displacement rate is 5×10^{-8} dpa/s, the dislocation density is 5×10^9 cm^{-2} and the void density is 8×10^{14} void/cm^3. The recombination number is 100 and the lattice parameter is 0.28 nm.
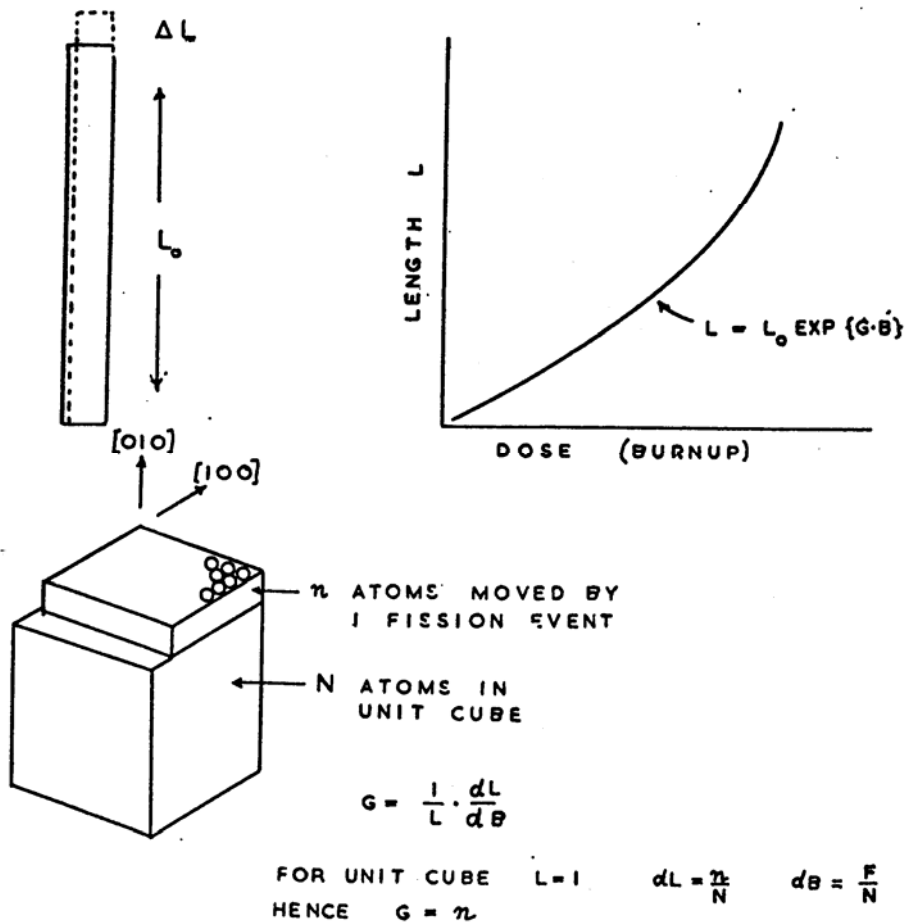
a) Calculate the swelling rate in % per dpa, in the absence of recombination.
b) Re-calculate taking into account the effect of recombination and compare.

27.2 A model for irradiation growth in U is based on the collapse of displacement cascades into interstitial loops with Burgers vectors parallel to 010 and vacancy loops with Burgers vectors parallel to 100. Derive an expression for the single crystal growth strain (cm/cm) along the 010 direction due to this mechanism as a function of neutron fluence. Each cascade involves n_a atoms, of which a fraction f goes into the loops after cascade collapse, the rest undergoing instantaneous recombination. Assume no annealing takes place and evaluate numerically for a fluence of 5×10^{21} (n.cm^{-2}), n_a =500, a=0.5 nm, f=10^{-3}, and σ_S=2b.

27.3. A fuel rod has been irradiated for three cycles to a neutron fluence of 10^{22} n.cm-2 (E > 1 MeV). Calculate the growth strains along the transverse, rolling and normal direction in the polycrystalline Zircaloy cladding , if the Kearns factors are F_T=0.1, F_R=0.4 and F_N=0.5. It is given that one in every 10^4 atoms that are displaced from the lattice contributes to the permanent growth strain
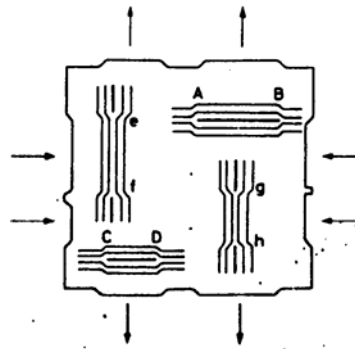
AERE - R 5262   Fig. 7a
Illustrating how planar clusters of inter-
stitial atoms and vacancies produce
macroscopic crystal distortion.

ΔL

L_o

[010]

[100]

LENGTH L

$L = L_o \, EXP \, \{G \cdot B\}$

DOSE   (BURNUP)

n ATOMS MOVED BY
I FISSION EVENT

N ATOMS IN
UNIT CUBE

$$G = \frac{I}{L} \cdot \frac{dL}{dB}$$

FOR UNIT CUBE   L=I $dL = \frac{n}{N}$ $dB = \frac{F}{N}$
HENCE   G = n

References for Chapter 27

[1]   D. H. Gurinsky and G. J. Dienes, "Nuclear Fuels," . New York: D. Van Nostrand, 1956.

[2]   S. H. Paine and J. H. Kittel, "Irradiation Effects in Uranium and its Alloys," presented at International Conference on Peaceful Uses of Atomic Energy, Geneva, 1955.

[3]   S. N. Buckley, "Iradiation Growth in Uranium," Atomic Energy Research Establishment, Harwell, England AERE R 5262, 1966.

[4]   S. N. Buckley, "Irradiation Growth," Atomic Energy Research Establishment, Harwell, England ARE-R 3674, 1961.

[5]   J. A. Horak and H. V. Rhude, "Irradiation Growth of Zirconium-Plutonium Alloys," *Journal of Nuclear Materials*, vol. 3, pp. 111-112, 1961.

[6]   V. Fidleris, "Irradiation Growth," Atomic Energy of Canada Ltd. AECL 7053, 1980.

[7]   M. Griffiths, *Journal of Nuclear Materials*, vol. 159, pp. 190-218, 1988.

[8]   C. H. Woo, "Effects of Anisotropic Diffusion on Irradiation Deformation," presented at 13th Radiation Efefct on Mtareials Symposium, 1986.

[9]   C. Cawthorne and J. E. Fulton, *Nature*, vol. 216, pp. 515-517, 1967.

[10]   J. S. Straalsund, R. W. Powell, and B. A. Chin, *Journal of Nuclear Materials*, vol. 108-109, pp. 299-305, 1982.

[11]   F. Garner, "Irradiation Performance of Cladding and Structural Steels in Liquid Metal Reactors," in *Nuclear Materials*, vol. 10A, *Materials Science and Technology*, B.R.T.Frost, Ed. Weinheim: VCH, 1994, pp. 419-557.

[12]   D. Faulkner and C. H. Woo, *Journal of Nuclear Materials*, vol. 90, pp. 307-316, 1980.

[13]   T. H. Courtney, *Mechanical Behavior of Materials*. New York: McGraw-Hill, 1990.

[14]   A. G. Evans, *Progress in Materials Science*, vol. 21, pp. 171, 1976.

[15]   M. F. Ashby, *Acta Metallurgica*, vol. 20, pp. 887, 1972.

[16]   XXX, "SIPA Creep reference," .